



## Trends in atmospheric ammonia at urban, rural and remote sites across North America

Xiaohong Yao<sup>1\*</sup>, Leiming Zhang<sup>2</sup>

<sup>1</sup> Lab of Marine Environmental Science and Ecology, Ministry of Education,  
Ocean University of China, Qingdao 266100, China

<sup>2</sup> Air Quality Research Division, Science and Technology Branch, Environment and  
Climate Change Canada, 4905 Dufferin Street, Toronto, Ontario, M3H 5T4, Canada

\*Corresponds to: Xiaohong Yao ( xhyao@ouc.edu.cn)



1    **Abstract.** Interannual variabilities in atmospheric ammonia ( $\text{NH}_3$ ) during the most  
2    recent seven to eleven years were investigated at fourteen sites across North America  
3    using the monitored data obtained from NAPS, CAPMoN and AMoN networks. The  
4    long-term average of atmospheric  $\text{NH}_3$  ranged from 0.8 to 2.6 ppb, depending on  
5    location, at four urban and two rural/agriculture sites in Canada. The annual average  
6    at these sites did not show any decreasing trend with largely decreasing anthropogenic  
7     $\text{NH}_3$  emission. An increasing trend was actually identified from 2003 to 2014 at the  
8    downtown Toronto site using either the Mann-Kendall or the Ensemble Empirical  
9    Mode Decomposition method, but “no” or “stable” trends were identified at other  
10   sites. The ~20% increase during the 11-year period at the site was likely caused by  
11   changes in  $\text{NH}_4^+/\text{NH}_3$  partitioning and/or air-surface exchange process as a result of  
12   the decreased sulfur emission and increased ambient temperature. The long-term  
13   average from 2008 to 2015 was 1.6-4.9 ppb and 0.3-0.5 ppb at four rural/agriculture  
14   and at four remote U.S. sites, respectively. A stable trend in  $\text{NH}_3$  mixing ratio was  
15   identified at one rural/agricultural site while increasing trends were identified at three  
16   rural/agricultural (0.6-2.6 ppb, 20-50% increase from 2008-2015) and four remote  
17   sites (0.3-0.5 ppb, 100-200% increase from 2008-2015). Increased ambient  
18   temperature was identified to be a cause for the increasing trends in  $\text{NH}_3$  mixing ratio  
19   at four out of the seven U.S. sites, but what caused the increasing trends at other U.S.  
20   sites needs further investigation.

21

22    **Keywords:** Gas-particle partitioning, reduced nitrogen, Ensemble Empirical Mode



23 Decomposition, climate impact.

24

## 25 **1. Introduction**

26 Atmospheric ammonia ( $\text{NH}_3$ ) plays an important role in formation of ammonium  
27 sulfate/nitrate aerosols in the size range of nanometer to supermicron (Kulmala et al.,  
28 2004; Ianniello et al., 2011; Yao and Zhang, 2012; Schiferl et al., 2014; Paulot and  
29 Jacob, 2014). The sum of sulfate, nitrate and ammonium ions ( $\text{NH}_4^+$ ) usually consist  
30 of the major portion of  $\text{PM}_{2.5}$  across Canada and the U.S. (Dabek-Zlotorzynska et al.,  
31 2011; Hand et al., 2012). With significant decreases in acidic gas emissions in the last  
32 decades across North America, e.g., emissions of  $\text{SO}_2$  and  $\text{NO}_x$  in Canada decreased  
33 from  $2.28 \times 10^6$  and  $2.72 \times 10^6$  tones/year in 2003 to  $1.23 \times 10^6$  and  $2.06 \times 10^6$  tones/year  
34 in \_\_\_\_\_ 2013, \_\_\_\_\_ respectively,  
35 (<http://www.ec.gc.ca/inrp-npri/donnees-data/ap/index.cfm?lang=En>), more attentions  
36 are paid to the relationship between  $\text{NH}_3$  and  $\text{NH}_4^+$  aerosols (Zhang et al., 2010; Day  
37 et al., 2012; Nowak et al., 2012; Yao and Zhang, 2012; Schiferl et al., 2014; Zhu et al.,  
38 2013; Markovic et al., 2014; Paulot and Jacob, 2014).

39

40  $\text{NH}_3$  mixing ratios are affected by several factors such as  $\text{NH}_3$  emissions,  $\text{NH}_3/\text{NH}_4^+$   
41 partitioning, and meteorological conditions (Sutton et al., 2009; Yao and Zhang, 2013;  
42 Hu et al., 2014). In Europe, previous studies showed that the long-term trend in  
43 atmospheric  $\text{NH}_3$  observed in some countries didn't show a decrease with a dramatic  
44 decrease in  $\text{NH}_3$  emissions and the phenomena was referred as "Ammonia Gap"



45 (Sutton et al., 2009; Ferm and Hellsten, 2012). Long-term trends in atmospheric NH<sub>3</sub>  
46 across North America are poorly understood (Zbieranowski and Aherne, 2011; Hu et  
47 al., 2104; Van Damme et al., 2014). Such knowledge is important for accurate  
48 prediction of ammonium sulfate/nitrate aerosol levels in the future (Pye et al., 2009;  
49 Walker et al., 2012). In North America, established anthropogenic NH<sub>3</sub> emission  
50 inventories showed that agricultural emissions accounted for over 80% of the total  
51 anthropogenic NH<sub>3</sub> emissions (Lillyman et al., 2009; Behera et al., 2013; Xing et al.,  
52 2013). However, agricultural emission sources only affect mixing ratios of  
53 atmospheric NH<sub>3</sub> at short downwind distances (Theobald et al., 2012; Yao and Zhang,  
54 2013). Non-agriculture emissions such as those from local traffics, waste containers  
55 and soil/vegetation were reported to be important contributors to NH<sub>3</sub> in urban  
56 atmospheres (Whitehead et al., 2007; Ellis et al; 2011; Reche et al., 2012; Sutton et al.,  
57 2013; Yao et al., 2013, Hu et al., 2014), although these sources only accounted for a  
58 few percentages of the total NH<sub>3</sub> emissions in Canada and the U.S. Due to new  
59 technology adopted, traffic-derived NH<sub>3</sub> decreased gradually (Bishop et al., 2010;  
60 <http://www.ec.gc.ca/inrp-npri/donnees-data/ap/index.cfm?lang=En>). Yao et al. (2013)  
61 and Hu et al (2014) recently reported that the traffic-derived NH<sub>3</sub> was a negligible  
62 contributor to atmospheric NH<sub>3</sub> in Toronto. However, under climate warming,  
63 soil/vegetation NH<sub>3</sub> emissions are expected to increase accordingly, e.g., NH<sub>3</sub>  
64 volatilization potential nearly doubles under every 5° C increase (Pinder et al., 2012;  
65 Sutton et al., 2013).

66



67 Atmospheric  $\text{NH}_3$  and ammonium sulfate/nitrate aerosols can be transported  
68 downwind and eventually deposited to natural ecosystems to enhance carbon fixation.  
69 Excessive  $\text{NH}_3$  deposition may cause adverse effects such as reduced biodiversity and  
70 eutrophication (Krupa et al., 2003; Erisman et al., 2007; Beem et al., 2010; Bobbink et  
71 al., 2010; Pinder et al., 2012). Recent evidence shows changes in species composition  
72 for sensitive vegetation types at the annual average concentration of  $1 \mu\text{g m}^{-3} \text{NH}_3$   
73 (Cape et al., 2009). Climate warming may increase the vulnerability of ecosystems  
74 towards exposure to  $\text{NH}_3$ . Thus, trend analysis of atmospheric  $\text{NH}_3$  at remote sites will  
75 help to better understand its potential impacts on sensitive natural eco-systems.

76

77 In this paper, interannual variabilities in atmospheric  $\text{NH}_3$  at fourteen sites across  
78 Canada and the U.S. were investigated, with particular attention paid to its long-term  
79 trends and causes. The fourteen sites include four urban sites, four remote sites and  
80 six rural/agriculture sites distributing at different latitudes. Two trend analysis tools,  
81 i.e., the Mann-Kendall (M-K) analysis (Gilbert, 1987) and the Ensemble Empirical  
82 Mode Decomposition (EEMD, Wu et al., 2009), were used to resolve the time series  
83 of atmospheric  $\text{NH}_3$  in mixing ratio at these sites. The analysis results provided new  
84 light on the long-term trends in atmospheric  $\text{NH}_3$  at various sites across North  
85 America.

86

## 87 2. Methodology

88 In this study, mixing ratios of atmospheric  $\text{NH}_3$  generated at monthly interval were



89 compiled from three data sources, i.e., the National Air Pollution Surveillance (NAPS,  
90 <http://www.ec.gc.ca/rnspa-naps/>) network, the Canadian Air and Precipitation  
91 Monitoring Network (CAPMoN), and the Passive Ammonia Monitoring Network  
92 (AMoN, <http://nadp.sws.uiuc.edu/nh3Net>). Missing data is a common problem during  
93 long-term observations. The sites chosen in this study were based on data  
94 availabilities as detailed below.

95

96 The NAPS network is to provide accurate and long-term air quality data across  
97 Canada. At each site, a  $PM_{2.5}$  sampler equipped with denuders is used to measure  
98 concentrations of  $NH_3$  and acidic gases and particulate chemical components such as  
99  $pNH_4^+$  and  $pNO_3^-$  in  $PM_{2.5}$ . The sampler operates for a 24-hr duration on every third  
100 day. At a few sites, technical problems resulted in  $NH_3$  and  $pNH_4^+$  concentration data  
101 missing for several months. At four urban sampling sites and one rural/agriculture site  
102 (Fig. 1), the measurements allowed obtaining continuous time series of monthly  
103 averaged concentrations of atmospheric  $NH_3$  and  $pNH_4^+$  and were thereby used for  
104 trend analysis. However, these sites also suffer from the problem of missing data. For  
105 example, there was only ~70% months when 8-10 sets of 24-hr data were available to  
106 calculate the monthly average value. In a few months, there were only 1-3 sets of  
107 24-hr data available to do so. This may cause uncertainty on the calculated trends in  
108 atmospheric  $NH_3$  and  $pNH_4^+$ . Moreover, one site at Egbert in the southern Ontario  
109 (Fig. 1), the part of CAPMoN, also had the long-term measurement concentrations of  
110 atmospheric  $NH_3$  and  $pNH_4^+$  using the identical sampler as used in the NAPS network.



111 The site is located at a rural/agriculture area. The data was also averaged monthly for  
112 the trend analysis. The six Canadian sites were referred as Sites 1-6 on basis of their  
113 annual average mixing ratios of atmospheric  $\text{NH}_3$  in decreasing order.

114

115 The AMoN within the National Atmospheric Deposition Program in the U.S. started  
116 operation in fall 2007. An important objective of AMoN is to assess long-term trends  
117 in  $\text{NH}_3$  concentrations and its deposition. AMoN included only sixteen sites in 2007  
118 and dozens of sites are now available. The Radiello® passive samplers are deployed  
119 every two weeks at each site according to the standard operating procedure for  
120 monitoring atmospheric  $\text{NH}_3$ . Puchalski et al. (2015) recently compared the bi-weekly  
121 passive measurements with those measured by annular denuder systems (ADS) at  
122 several AMoN sites and found that the mean relative percentage difference between  
123 the ADS and AMoN sampler was -9%. In this study, mixing ratios of atmospheric  
124  $\text{NH}_3$  at eight AMoN's sites were selected for the trend analysis on basis of two criteria  
125 (Fig 1): 1) the length of the valid data should be at least seven years according to  
126 Walker et al., (2000); and 2) there were no monthly average data missing in each year.  
127 The eight sites were referred as Site 7-14 (Fig 1), four of which were located at rural  
128 areas and another four at remote areas. Consistent with the six sites across Canada, the  
129 monthly averages at the eight sites were used for data analysis if not specified.  
130 Moreover, all ambient temperature (T) data were obtained from on-site records or  
131 nearby meteorological stations.

132



133 The M-K analysis is a non-parametric statistical procedure which can be used to  
134 analyze trends in data sets including irregular sampling intervals, data below the  
135 detection limit, and trace or missing data (Kampata et al., 2008). Considering the data  
136 flaws aforementioned were indeed presented in our selected datasets to different  
137 extents, the M-K analysis is thereby used to resolve the time series of the annual  
138 average of  $\text{NH}_3$  in this study. The M-K method yields qualitative trend results such as  
139 “increasing/decreasing”, “probable increasing/decreasing”, “stable” and “no trend”,  
140 depending on the calculated “S” statistic, confidence factor and coefficient of  
141 variation (Gilbert, 1987). Moreover, the EEMD is a recently developed statistical tool  
142 to determine the trend of a time series of a variable in various fields such as  
143 economics, health, environment and climate (Wu et al., 2009). The EEMD built on  
144 Empirical Mode Decomposition (EMD) and was updated by Wu et al. (2009) to  
145 overcome the problem of mode mixing in the EMD. The method has since been  
146 applied widely (e.g., Erturk et al., 2103; Ren et al., 2014) because it is most suitable  
147 for resolving non-stationary and non-linear signals. The mixing ratio of atmospheric  
148  $\text{NH}_3$  was affected not only by its emissions, atmospheric transport, dilution and  
149 deposition, but also affected by non-stationary and non-linear chemical reactions  
150 (Ianniello et al., 2011; Hu et al., 2014). Thus, the EEMD is also used in this study and  
151 is briefly introduced here.

152 In general, all data are amalgamations of signal and noise as shown below:

$$153 X(t)=S(t)+N(t)$$

154 where  $X(t)$  is the record data, and  $S(t)$  and  $N(t)$  are the true signal and noise,





155 respectively. In the EMD, any dataset is assumed to consist of different simple  
156 intrinsic modes of oscillations. Each of these intrinsic oscillatory modes is represented  
157 by an intrinsic mode function (IMF). In the EEMD, white noise is added to the single  
158 data set,  $X(t)$ , and the ensemble mean is used to improve accuracy of measurements.

159

### 160 **3. Results and discussion**

#### 161 *3.1 Temporal variations of atmospheric $\text{NH}_3$ at the six Canadian sites*

162 Fig. 2 shows monthly variations of atmospheric  $\text{NH}_3$  in mixing ratio at the six  
163 Canadian sites. At Site 1, an urban site in downtown Toronto, the measured mixing  
164 ratios were  $2.6 \pm 1.2$  ppb (average  $\pm$  standard deviation) during the period from July  
165 2003 to June 2014 (Fig 2a and Table 1). When compared with those reported in other  
166 urban atmospheres, the long-term average value of 2.6 ppb ranked at a moderately  
167 low concentration level (Whitehand et al., 2007; Saylor et al., 2010; Alebic-Juretic,  
168 2008; Meng et al., 2011). Interannual variations were evident at Site 1 with the  
169 coefficient of variation (CV) of 0.11, defined as the ratio of the standard deviation to  
170 the average. It should be noted that the annual averages in 2004 and 2005 were  
171 calculated from July 2003 to June 2004 and from July 2004 to June 2005, respectively,  
172 instead of a calendar year, in order to obtain the longest time series of annual averages.  
173 The similar calculations were used for other years and other sites. The M-K analysis  
174 result suggested an increasing trend from 2004 to 2014 with a confidence level of  
175 98%. When intra-annual variations were analyzed at Site 1, a distinctive seasonal  
176 trend was obtained with the highest seasonal average value of  $3.7 \pm 0.7$  ppb in summer



177 (June to August) and the lowest of  $1.3 \pm 0.6$  in winter (December to the next February).

178

179 The M-K analysis results showed either “no” or “stable” trends in atmospheric  $\text{NH}_3$  at  
180 the other Canadian sites with long-term average of  $2.4 \pm 0.6$  ppb at Site 2,  $2.1 \pm 1.2$  ppb  
181 at Site 3,  $1.9 \pm 0.8$  ppb at Site 4,  $1.6 \pm 0.5$  ppb at Site 5, and  $0.8 \pm 0.6$  ppb at Site 6 (Fig.  
182 2b-f). However, interannual variations at these sites were evident, e.g., the CV values  
183 calculated from annual averages varied from 0.07 to 0.19, depending on location  
184 (Table 1). Atmospheric  $\text{NH}_3$  at Sites 3, 4 and 6 exhibited a distinctive seasonal  
185 variation, but this was not the case at Sites 2 and 5. The largest seasonal variation  
186 occurred at Site 3 while the smallest occurred at Site 2. The two sites were selected as  
187 examples for further discussion below.

188

189 Site 3 is situated at a rural/agriculture area in Saint-Anicet of Quebec. The largest  
190 seasonal average value occurred in the fall during the measurement period of  
191 September 2003 - August 2014. Fertilizer application usually leads to a sharp increase  
192 in atmospheric  $\text{NH}_3$  mixing ratio (Lillyman et al., 2009; Yao and Zhang, 2013) and  
193 this was indeed observed at Site 3. For example, there was usually one 24-hr sample  
194 in October having a mixing ratio 1-2 orders of magnitude higher than other samples  
195 collected before or after (figure not shown). The on-site sampling was performed  
196 every third day, and strong  $\text{NH}_3$  emissions associated with fertilization application  
197 generally occurred within the initial 3-5 days (Lillyman et al., 2009). Thus,  
198 extremely high mixing ratios could be observed on one day in October in some years,



199 but not in every year. The episodes further led to large interannual variations with the  
200 value of CV reached 0.19.

201

202 Site 2 is located at an urban area in Edmonton. Mixing ratios of atmospheric NH<sub>3</sub>  
203 were 2.4±0.6 ppb and the differences between seasonal average values were only  
204 0.1-0.3 ppb during the period of May 2006 - April 2014. However, the seasonal  
205 average temperature of 16.7±1.9°C in summer was much higher than that of  
206 -19.8±4.5 °C in winter. Soil/vegetation NH<sub>3</sub> emissions should be negligible in such  
207 cold winters, however, industrial and/or non-industrial anthropogenic sources might  
208 be enhanced in winter, which could explain the small seasonal variations in NH<sub>3</sub>  
209 mixing ratio at this site. This hypothesis was supported by the much higher (2.0-4.0  
210 times) mixing ratios of SO<sub>2</sub>, HONO and HNO<sub>3</sub> in winter as compared to those in  
211 summer (figure not shown).

212

### 213 *3.2 Temporal variations of atmospheric NH<sub>3</sub> at the eight American sites*

214 For the eight AMoN's sites in the U.S., the data measured from August 2008 to July  
215 2015 were used for analysis at all the sites except at Site 12 for which the data  
216 measured during the period of September 2008 - August 2015 was used (Fig. 3 and  
217 Table 1). Site 7 is located at an intensive agriculture activity zone in Randall of Taxes,  
218 and Sites 8-10 are located at rural areas in Dodge of Wisconsin, Wayne of Michigan,  
219 and Champaign of Illinois, respectively, with moderately intensive agriculture  
220 activities. Long-term average of NH<sub>3</sub> was as high as 4.9±1.2 ppb at Site 7 where the



221 seasonal average in summer was approximately 20% higher than those in the other  
222 seasons. The M-K analysis result showed an increasing trend at this site with a  
223 confidence level of 99.9%. Long-term average of  $\text{NH}_3$  at Sites 8-10 were  $2.6 \pm 1.4$ ,  
224  $2.2 \pm 1.0$  and  $1.6 \pm 1.0$  ppb, respectively, and distinctive seasonal variations were seen at  
225 the three sites with the lowest values in winter. The M-K analysis results showed an  
226 increasing trend at Sites 9-10 with a confidence level of  $>98\%$  and no trend at Site 8.

227

228 Sites 11-14 are located at the remote areas in Tompkins of New York, Lake of  
229 Minnesota, Charleston of South Carolina, and Rio Arriba of New Mexico,  
230 respectively. The long-term average  $\text{NH}_3$  was only 0.3-0.5 ppb at these four remote  
231 sites, but with distinctive seasonal variations with the highest in summer and the  
232 lowest in winter (Table 1). The M-K analysis results showed an increasing trend at the  
233 four sites with a confidence level of  $>95\%$ .

234

### 235 *3.3 Exponential correlations between $\text{NH}_3$ and T*

236 When local soil/vegetation emissions were the major contributors to atmospheric  $\text{NH}_3$ ,  
237 its mixing ratio usually exhibited as an exponential function of ambient T (Sutton et  
238 al., 2009; Flechard et al., 2013; Hu et al., 2014). Thus, the exponential correlation  
239 relationship was examined at the fourteen sites to identify potential major contributors  
240 to atmospheric  $\text{NH}_3$ . Note that a perfect exponential correlation with  $R^2 > 0.9$  would  
241 occur only when the soil/air mass transfer of  $\text{NH}_3$  was not the limitation factor  
242 (Flechard et al., 2013; Hu et al., 2014), and soil/air mass transfer rate associated with



243 dry soil was much small (Su et al., 2011).

244

245 A moderately good exponential correlation was obtained at Site 1 with  $R^2=0.74$  and P  
246 value  $<0.01$  (Fig. S1a).  $\text{NH}_3$  emissions from green space surrounding this site likely  
247 played a major role in the observed  $\text{NH}_3$  level (Hu et al., 2014). Similar results were  
248 obtained at Sites 3, 4 and 6 when a few exterior data points were excluded. For  
249 example, five data points at Site 3 severely deviate from the regression curve because  
250 of fertilizer application (Fig. S1c). When these five data points were excluded,  $R^2$   
251 reached 0.60 and P value  $<0.01$ . In addition,  $R^2$  was 0.75 at the rural Site 6 when one  
252 outlier data point was excluded (Fig. S1f). The two parameters in the regression  
253 equation  $[\text{NH}_3]=0.24*\exp(0.094*T)$  were largely different from those obtained at the  
254 two downtown sites, i.e.,  $[\text{NH}_3]=1.48*\exp(0.048*T)$  at Site 1 and  
255  $[\text{NH}_3]=1.29*\exp(0.036*T)$  at Site 4, noting that the parameters were close between  
256 the two downtown sites. Under the condition of T below or close to  $0^\circ\text{C}$ , the mixing  
257 ratios of atmospheric  $\text{NH}_3$  at the rural Site 6 were almost one order of magnitude  
258 smaller than those at the downtown sites, leading to the large difference for  
259 parameters in regression equations between the rural and urban sites. The higher  
260 mixing ratio under freezing condition at the Toronto downtown site was proposed to  
261 be likely associated with  $\text{NH}_3$  emissions from green space (Hu et al., 2014). Flechard  
262 et al (2013) also reported a higher  $\text{NH}_3$  emission from grassland under freezing  
263 condition, but the corresponding mechanism is still not clear.

264



265 At Site 2, the exponential correlation was poor even with two outlier samples being  
266 excluded (Fig. S1b), implying that local soil/vegetation emissions were less likely the  
267 major contributors to atmospheric  $\text{NH}_3$ . Like Site 2,  $R^2$  was only 0.39 at Site 5 even  
268 with two exterior data points being excluded (Fig. S1e).  $\text{NH}_3$  in urban atmospheres  
269 were reported to come from various sources (Whitehead et al., 2007; Ianniello et  
270 al., 2010; Saylor et al., 2010; Meng et al., 2011; Reche et al., 2012), some of which  
271 were less dependent on ambient T.

272

273  $R^2$  between atmospheric  $\text{NH}_3$  and ambient T was below 0.1 at Site 7 (Fig S2a).  
274 Considered the high mixing ratios observed at the rural/agriculture site, it can be  
275 confirmed that local agriculture emissions were the major contributor to atmospheric  
276  $\text{NH}_3$  and the agriculture emissions appeared to be independent on ambient T.  $R^2$  of  
277 0.64, 0.69 and 0.45 at Sites 8-10, respectively, (Fig. S2b-d) suggested that local  
278 soil/vegetation emissions should be among the major contributors to atmospheric  $\text{NH}_3$ .  
279 The same can be said for the remote Site 11 with  $R^2$  of 0.63 (Fig. S2e).  $R^2$  was 0.25,  
280 0.2 and 0.15 at remote Sites 12-14 (Fig S2f-i), respectively. When the data measured  
281 in calendar year 2011, 2012, 2013 and 2014 at Site 13 were used for correlation  
282 analysis, respectively; the values of  $R^2$  were 0.47 in 2011, 0.58 in 2012, 0.69 in 2013  
283 and 0.74 in 2014. Local soil/vegetation emissions might be among the major  
284 contributors to atmospheric  $\text{NH}_3$  at the site while the low  $R^2$  values in 2011-2012  
285 could be due to analytical errors. In fact, the mixing ratios at the site in 2011-2012  
286 were generally close to the detection limit. A similar calculation was conducted at Site



287 14 with  $R^2$  still below 0.2 in different calendar years, suggesting that local  
288 soil/vegetation emissions were unlikely the major contributors to atmospheric  $\text{NH}_3$ .  
289 Yao and Zhang (2013) proposed that long-range transport could be an important  
290 contributor to atmospheric  $\text{NH}_3$  at remote sites in North America. When a similar  
291 calculation was conducted at Site 12,  $R^2$  was 0.57 in 2012, 0.81 in 2013 and 0.39 in  
292 2014. Local soil/vegetation emissions were possibly among the major contributors to  
293 atmospheric  $\text{NH}_3$  at the site in 2012 and 2013, but the long-range transport together  
294 with local soil/vegetation emissions might be important contributors to atmospheric  
295  $\text{NH}_3$  in 2014.

296

### 297 *3.4 Cause analysis of trends in atmospheric $\text{NH}_3$ at Canadian sites*

298 Site 1 is located in Downtown Toronto, Ontario. Fig S3a shows the annual  
299 anthropogenic  $\text{NH}_3$  emissions from 2003 to 2013 in Ontario, Canada. Not only the  
300 total  $\text{NH}_3$  emissions, but also emissions from the four major sectors including  
301 agriculture, mobile, industrial and non-industrial generally decreased. However, an  
302 increasing trend in annual average  $\text{NH}_3$  was found at Site 1, which was identified to  
303 be caused by (1) the increased T, and (2) the decreased  $\text{SO}_2$  emission. Increasing T not  
304 only increases soil/vegetation  $\text{NH}_3$  emissions but also affects  $\text{NH}_3/\text{pNH}_4^+$  partitioning,  
305 both processes would increase  $\text{NH}_3$  mixing ratios. The decreased  $\text{SO}_2$  emissions due  
306 to the tightened emission control policies since 2008 by the city and provincial  
307 governments led to significant declines in  $\text{SO}_2$  oxidation products (Hu et al., 2014;  
308 Pugliese et al 2014), which in turn also affected  $\text{NH}_3/\text{pNH}_4^+$  partitioning and



309 increased  $\text{NH}_3$  mixing ratios. These hypotheses were supported by the trends in T and  
310  $\text{pNH}_4^+$  and their correlations with that in  $\text{NH}_3$ , as detailed below.

311

312 A moderately good correlation ( $R^2=0.76$ , P value  $<0.01$ ) was obtained between the  
313 annual average  $\text{NH}_3$  and the annual average T, while a negative correlation ( $R^2=0.40$   
314 and P value  $<0.05$ ) was obtained between the annual average  $\text{NH}_3$  and  $\text{pNH}_4^+$  (Fig.  
315 4a). Note that a decreasing trend in annual average  $\text{pNH}_4^+$  was found with a  
316 confidence level of  $>99\%$  based on M-K analysis. When ambient T was increased by  
317  $5^\circ\text{C}$ , the mixing ratio of atmospheric  $\text{NH}_3$  was increased by  $\sim 1$  ppb according to the  
318 regression equation.

319

320 Fig. S4 shows the intrinsic mode functions (IMFs) and residuals solved by the EEMD  
321 at Site 1. The extracted residuals represented the long-term trend in atmospheric  $\text{NH}_3$   
322 and the IMFs represented other fluctuations in different time scales. The  
323 EEMD-extracted long-term trend in atmospheric  $\text{NH}_3$  was generally increased by  $\sim 20\%$   
324 from 2003 to 2014. The EEMD was also used to extract the long-term trend in  $\text{pNH}_4^+$   
325 in  $\text{PM}_{2.5}$  from 2003 to 2014 (Fig. S5). Correlation between the two EEMD-extracted  
326 long-term trends resulted in a regression equation of  $[\text{NH}_3] = -1.41 * [\text{pNH}_4^+] + 4.3$ ,  
327 with  $R^2=0.93$  and P value  $<0.01$  (Figure 4b). The unit of  $\text{NH}_3$  is in ppb while the unit  
328 of  $\text{pNH}_4^+$  is in  $\mu\text{g m}^{-3}$ . The absolute value of the regression slope was almost the same  
329 as the unit conversion coefficient. Thus, the EEMD-extracted long-term trend in  
330 atmospheric  $\text{NH}_3$  seemed to be mainly determined by the change in  $\text{NH}_3/\text{pNH}_4^+$





331 partitioning. The increasing T further enhanced this trend. When the EEMD-extracted  
332 long-term trend in ambient T was correlated to that of atmospheric NH<sub>3</sub>, we obtained  
333 [NH<sub>3</sub>] = 0.13\*T+1.5, R<sup>2</sup>=0.47 and P value <0.01 (Fig 4b). The EEMD-extracted  
334 results suggest that the changes in NH<sub>3</sub>/NH<sub>4</sub><sup>+</sup>partitioning is one of the dominant  
335 factors influencing the long-term NH<sub>3</sub> trend at Site 1. The relative importance  
336 between (1) changes in NH<sub>3</sub>/NH<sub>4</sub><sup>+</sup>partitioning and (2) increased biogenic NH<sub>3</sub>  
337 emission due to increasing T is yet to be investigated.

338

339 At Site 2, the EEMD-extracted residual of atmospheric NH<sub>3</sub> varied within a very  
340 small range (~10%, Fig. 5), which was consistent with stable trend generated from the  
341 M-K analysis. Little correlation was found between the annual average NH<sub>3</sub> and T  
342 (R<sup>2</sup><0.05) or pNH<sub>4</sub><sup>+</sup> (R<sup>2</sup><0.01). Thus, the NH<sub>3</sub> trend identified at Site 2 was seemingly  
343 unaffected by changes in NH<sub>3</sub>/NH<sub>4</sub><sup>+</sup>partitioning and T-dependent biogenic NH<sub>3</sub>  
344 emission, or additional local factors cancelled out the impact from the two factors.

345

346 Site 3 is a rural/agriculture site and annual agriculture NH<sub>3</sub> emissions in Quebec were  
347 stable from 2003 to 2009 with CV of 0.02 (Fig S3b). During the same period, mobile,  
348 industrial and non-industrial emissions were decreased by 40% in Quebec. While the  
349 M-K analysis result showed no consistent long-term trend in atmospheric NH<sub>3</sub>, the  
350 EEMD-extracted a bell-shaped pattern (Fig. 5), i.e., NH<sub>3</sub> increased from 1.7 ppb in  
351 2003 to 2.5 ppb in 2009 and then decreased down to 1.3 ppb in 2014. The  
352 anthropogenic NH<sub>3</sub> emission data from 2003 to 2009 didn't support the increasing



353 trend in atmospheric NH<sub>3</sub> at this site during this period.

354

355 A good correlation was found between the EEMD-extracted long-term trends in NH<sub>3</sub>  
356 and T with a linear regression relationship of  $[\text{NH}_3] = 0.39 \cdot T - 0.30$ , with  $R^2=0.80$   
357 and P value  $<0.01$ . The slope of 0.39 was consistent with that reported by Sutton et al  
358 (2013), i.e., NH<sub>3</sub> volatilization potential nearly doubles every 5°C. On the contrary,  
359 little correlation was found between the EEMD-extracted residuals for atmospheric  
360 NH<sub>3</sub> and pNH<sub>4</sub><sup>+</sup> ( $R^2<0.1$ ), suggesting that the NH<sub>3</sub>/pNH<sub>4</sub><sup>+</sup> partitioning likely played a  
361 negligible role on the long-term trend in atmospheric NH<sub>3</sub> at this site. The increasing  
362 trend in NH<sub>3</sub> should mainly be caused by increased biogenic NH<sub>3</sub> emission due to the  
363 increased T.

364

365 A similar conclusion could also be generated for Site 4 to that for Site 3. The M-K  
366 analysis results showed a stable trend in atmospheric NH<sub>3</sub> and a slightly decreasing  
367 trend in pNH<sub>4</sub><sup>+</sup> with a confidence level of  $>99\%$ . The EEMD-extracted long-term  
368 trend showed that NH<sub>3</sub> decreased by  $\sim 5\%$  from 2007 to 2008 and then increased by  
369  $\sim 50\%$  afterwards. Although the correlation between the annual averages NH<sub>3</sub> and T  
370 was not very good ( $R^2=0.39$ ,  $P=0.13$ ), correlation between the EEMD-extracted  
371 long-term trends in NH<sub>3</sub> and T was almost perfect ( $R^2= 0.90$ ,  $P<0.01$ ). No correlation  
372 was found between the annual average NH<sub>3</sub> and [pNH<sub>4</sub><sup>+</sup>] ( $R^2<0.01$ ), and a relatively  
373 low correlation was found between the EEMD-extracted long-term trends in  
374 atmospheric NH<sub>3</sub> and pNH<sub>4</sub><sup>+</sup> ( $R^2=0.39$ , P value  $<0.01$ ). These results suggested that



375 the long-term change in ambient T possibly dominated the long-term trend in  
376 atmospheric NH<sub>3</sub> at the site.

377

378 Site 5 is an urban site located in British Columbia, Canada. Anthropogenic NH<sub>3</sub>  
379 emissions were decreased from 2003 to 2013 in this province (Fig S3c). The M-K  
380 analysis result showed no trend in atmospheric NH<sub>3</sub> at Site 5 from 2003 to 2014 and  
381 the EEMD-extracted long-term trend was almost constant. Based on the correlation  
382 analysis of the EEMD-extracted results (not shown), the long-term changes in  
383 ambient T and pNH<sub>4</sub><sup>+</sup> cannot explain the EEMD-extracted trend in atmospheric NH<sub>3</sub>  
384 at this site.

385

386 At Site 6, the EEMD-extracted trend in atmospheric NH<sub>3</sub> showed an increase of ~10%  
387 from 2003 to 2006 and then a decrease of ~40% afterwards (Fig. 5). Poor correlations  
388 were found between annual average NH<sub>3</sub> and T or between NH<sub>3</sub> and NH<sub>4</sub><sup>+</sup> with P  
389 values >0.05. Meaningless correlations between the EEMD-extracted trends in NH<sub>3</sub>  
390 and T or between the EEMD-extracted trends in NH<sub>3</sub> and NH<sub>4</sub><sup>+</sup> were obtained. The  
391 trend in T and NH<sub>3</sub>/NH<sub>4</sub><sup>+</sup> partitioning cannot explain the long-term variations of  
392 atmospheric NH<sub>3</sub>.

393

### 394 *3.5 Cause analysis of trends in atmospheric NH<sub>3</sub> at the U.S. sites*

395 At the eight U.S. sites, R<sup>2</sup> between annual average NH<sub>3</sub> and T were all below 0.2 with  
396 P values all larger than 0.1. The simple correlation analysis did not provide direct



397 evidence that T was the dominant factor affecting the NH<sub>3</sub> trend. However, the  
398 EEMD-extracted trends in NH<sub>3</sub> and T had a much better correlation at some sites, e.g.,  
399 with R<sup>2</sup>= 0.85, 0.99, 0.54 and 0.99 at Site 7, 8, 9 and 13, respectively, and with P  
400 values small than 0.01. Thus, the increasing T should be one of the main factors  
401 causing the long-term trend in NH<sub>3</sub> at these four sites. Note that no reasonable  
402 relationship was identified between trends in NH<sub>3</sub> and T at the other four sites using  
403 the EEMD method.

404

405 The EEMD-extracted long-term trend showed an increase in atmospheric NH<sub>3</sub> from  
406 4.2 ppb in August 2008 to 6.8 ppb in July 2015 at Site 7 (Fig. 6a), from 2.4 ppb in  
407 August of 2008 to 3.0 ppb in July of 2015 at Site 8 (Fig. 6b), from 1.8 ppb in August  
408 of 2008 to 2.8 ppb in July of 2015 at Site 9 (Fig. 6c), a complex varying pattern  
409 during the period from August 2008 to July 2015 at Site 10 (Fig. 6d), and an  
410 increasing trend (by 0.3-0.5 ppb, or 100-200% in percentages) at Sites 11-14 (Fig.  
411 6e-h). The percentage increases (100-200%) in NH<sub>3</sub> mixing ratio from 2008 to 2015  
412 at the remote sites were substantially larger than those at the rural/agriculture sites  
413 (20-50%).

414

415 NH<sub>3</sub> emissions in the United States increased by 11 % during the period from 1990 to  
416 2010 due to the growth of livestock activities (Xing et al., 2013). This is particularly  
417 the case in North Carolina and Iowa. This increase along is not enough to explain the  
418 ~50% increase in NH<sub>3</sub> from 2008 to 2015 at Site 7 which is located in Texas. The



419 increased T is believed to be another important factor causing the increased NH<sub>3</sub> at  
420 this site as mentioned above. It is also noted that the increasing trends in NH<sub>3</sub> at Site  
421 11-14 identified using the EEMD-extracted results were also consistent with the M-K  
422 analysis results.

423

424 The annual average NH<sub>3</sub> at the remote sites reached 0.4-0.6 ppb in 2015. Assuming  
425 the same increasing rate continues for another 7-10 years, the annual average will  
426 exceed the proposed critical level of 1 µg m<sup>-3</sup> at two sites for protecting sensitive  
427 ecosystems (Cape et al., 2009).

428

#### 429 **4. Conclusions**

430 Long-term average of atmospheric NH<sub>3</sub> was in the range of 0.3-0.5, 1.6-2.6, and  
431 0.8-4.9 ppb at the remote, urban, and rural/agriculture sites, respectively, across the  
432 North America. Moderate exponential correlations between atmospheric NH<sub>3</sub> and  
433 ambient T were found at nine sites, implying that local biogenic emissions and/or  
434 NH<sub>3</sub>/NH<sub>4</sub><sup>+</sup> partitioning were likely dominant factors causing the long-term trends in  
435 atmospheric NH<sub>3</sub> at these sites.

436

437 At the four Canadian sites, no decreasing trends in atmospheric NH<sub>3</sub> were found  
438 despite significant decreases in anthropogenic NH<sub>3</sub> emissions from main sectors in the  
439 last decade. The decreased NH<sub>3</sub> anthropogenic emission was compensated or  
440 overwhelmed by the increased biogenic emission and/or changes in NH<sub>3</sub>/NH<sub>4</sub><sup>+</sup>



441 partitioning. This was supported by  $\text{pNH}_4^+$  data which exhibited a decreasing trend,  
442 likely caused by a combination of reduced  $\text{SO}_2$  and  $\text{NO}_x$  emission and increased  
443 temperature. No decreasing trends in atmospheric  $\text{NH}_3$  were found at other two  
444 Canadian sites, but it was unknown what caused this.

445

446 The M-K analysis showed an increasing trend in atmospheric  $\text{NH}_3$  at seven out of the  
447 eight U.S. sites, which was also supported by the EEMD-extracted results.  $\text{NH}_3$   
448 increased by 20-50% from 2008 to 2015 at the three rural/agriculture sites and by  
449 100%-200% at the four remote sites. If the same increasing trend continues in the next  
450 5-7 years, the annual average  $\text{NH}_3$  at two remote sites will exceed  $1 \mu\text{g m}^{-3}$ , a level  
451 below which has been proposed to protect sensitive eco-systems at the remote sites.

452

453 In most cases, the two statistical approaches used in the present study yield consistent  
454 trends in atmospheric  $\text{NH}_3$  measured at different sites. The EEMD method appeared  
455 to have more powerful interpretation ability for resolving trends because 1) it is less  
456 affected by extremely high concentration points, and 2) it yields a continuous and  
457 quantitative trend result. However, this method occasionally suffers from “the end  
458 effect” and leads to physically meaningless results. Using the combined (or more than  
459 one statistical methods) can better resolve and interpret long-term trends in  
460 atmospheric  $\text{NH}_3$ .

461

462 **Acknowledgement**



463 Ammonia Monitoring Network (<http://nadp.sws.uiuc.edu/data/sites/list/?net=AMoN>)  
464 is acknowledged for downloading data for analysis. The work is financially supported  
465 by the Clear Air Regulatory Agenda of Canada and xhy thanks the support from the  
466 National Program on Key Basic Research Project (973 Program: 2014CB953700) of  
467 China.

468

#### 469 Reference

- 470 Alebic-Juretic, A.: Airborne ammonia and ammonium within the Northern Adriatic  
471 area, Croatia, *Environ. Pollut.*, 154, 439-447, doi:10.1016/j.envpol.2007.11.029,  
472 2008.
- 473 Beem, K. B., Raja, S., Schwandner, F. M., Taylor, C., Lee, T., Sullivan, A. P., Carrico, C.  
474 M., McMeeking, G. R., Day, D., Levin, E., Deposition of reactive nitrogen during  
475 the Rocky Mountain Airborne Nitrogen and Sulfur (RoMANS) study. *Environ.*  
476 *Pollut.*, 158, 862-872, doi:10.1016/j.envpol.2009.09.023, 2010.
- 477 Behera, S. N., Sharma, M., Aneja, V. P., Balasubramanian, R.: Ammonia in the  
478 atmosphere: a review on emission sources, atmospheric chemistry and deposition  
479 on terrestrial bodies, *Environ. Sci. Pollut. Res.*, 20, 8092-8131,  
480 doi:10.1007/s11356-013-2051-9, 2013.
- 481 Bishop, G.A., Peddle, A.M., Stedman, D.H., Zhan, T.: On-road emission measurements  
482 of reactive nitrogen compounds from three California cities, *Environ. Sci.*  
483 *Technol.*, 44, 3616–3620, doi:10.1021/es903722p, 2010.
- 484 Bobbink, R., Hicks, K., Galloway, J., Spranger, T., Alkemade, R., Ashmore, M.,  
485 Bustamante, M., Cinderby, S., Davidson, E., Dentener, F.: Global assessment of  
486 nitrogen deposition effects on terrestrial plant diversity: a synthesis, *Ecol. Appl.*,  
487 20, 30-59, doi:10.1890/08-1140.1, 2010.
- 488 Cape, J. N., Van der Eerden, L. J., Sheppard, L. J., Leith, I. D., Sutton, M. A.: Evidence  
489 for changing the critical level for ammonia, *Environ. Pollut.*, 157, 1033-1037,  
490 doi:10.1016/j.envpol.2008.09.049, 2009.
- 491 Dabek-Zlotorzynska, E., Dann, T. F., Martinelango, P. K., Celio, V., Brook, J. R.,  
492 Mathieu, D., Ding, L., Austin, C. C.: Canadian National Air Pollution  
493 Surveillance (NAPS) PM<sub>2.5</sub> speciation program: methodology and PM<sub>2.5</sub>  
494 chemical composition for the years 2003-2008, *Atmos. Environ.*, 45, 673-686,  
495 doi:10.1016/j.atmosenv.2010.10.024, 2011.
- 496 Day, D. E., Chen, X., Gebhart, K. A., Carrico, C. M., Schwandner, F. M., Benedict, K.  
497 B., Schichtel, B. A., Collett, J. L.: Spatial and temporal variability of ammonia



- 498 and other inorganic aerosol species, *Atmos. Environ.*, 61, 490-498,  
499 doi:10.1016/j.atmosenv.2012.06.045, 2012.
- 500 Ellis, R. A., Murphy, J. G., Markovic, M. Z., VandenBoer, T. C., Makar, P. A., Brook, J.,  
501 Mihele, C.: The influence of gas-particle partitioning and surface-atmosphere  
502 exchange on ammonia during BAQS-Met, *Atmos. Chem. Phys.*, 11, 133-145,  
503 doi:10.5194/acp-11-133-2011, 2011.
- 504 Erisman, J.W., Bleeker, A., Galloway, J., Sutton, M. S.: Reduced nitrogen in ecology  
505 and the environment, *Environ. Pollut.*, 150, 140-149,  
506 doi:10.1016/j.envpol.2007.06.033, 2007.
- 507 Erturk, A., Gullu, M. K., Erturk, S.: Hyperspectral image classification using empirical  
508 mode decomposition with spectral gradient enhancement, *IEEE Trans. Geosci.*  
509 *Remot. Sens.*, 51, 2787-2798, doi:10.1109/TGRS.2012.2217501, 2013.
- 510 Ferm, M., Hellsten, S.: Trends in atmospheric ammonia and particulate ammonium  
511 concentrations in Sweden and its causes, *Atmos. Environ.*, 61, 30-39,  
512 doi:10.1016/j.atmosenv.2012.07.010, 2012.
- 513 Flechard, C. R., Massad, R., Loubet, B., Personne, E., Simpson, D., Bash, J. O., Cooter,  
514 E. J., Nemitz, E., Sutton, M. A.: Advances in understanding, models and  
515 parameterisations of biosphere-atmosphere ammonia exchange, *Biogeosciences*,  
516 10, 5183-5225, doi:10.5194/bg-10-5183-2013, 2013.
- 517 Gilbert, R.O.: *Statistical Methods for Environmental Pollution Monitoring*, John  
518 Wiley & Sons, 1987.
- 519 Hand, J. L., Schichtel, B. A., Pitchford, M., Malm, W. C., Frank, N. H.: Seasonal  
520 composition of remote and urban fine particulate matter in the United States, *J.*  
521 *Geophys. Res.-Atmos.*, 117, D05209, doi:10.1029/2011JD017122, 2012.
- 522 Hu, Q., Zhang, L., Evans, G. J., Yao, X.: Variability of atmospheric ammonia related to  
523 potential emission sources in downtown Toronto, Canada, *Atmos. Environ.*, 99,  
524 365-373, doi:10.1016/j.atmosenv.2014.10.006, 2014.
- 525 Ianniello, A., Spataro, F., Esposito, G., Allegrini, I., Hu, M., Zhu, T.: Chemical  
526 characteristics of inorganic ammonium salts in PM 2.5 in the atmosphere of  
527 Beijing (China), *Atmos. Chem. Phys.*, 11, 10803-10822,  
528 doi:10.5194/acp-11-10803-2011, 2011.
- 529 Ianniello, A., Spataro, F., Esposito, G., Allegrini, I., Rantica, E., Ancora, M. P., Hu, M.,  
530 Zhu, T.: Occurrence of gas phase ammonia in the area of Beijing (China), *Atmos.*  
531 *Chem. Phys.*, 10, 9487-9503, doi:10.5194/acp-10-9487-2010, 2010.
- 532 Kampata, J. M., Parida, B. P., Moalafhi, D. B.: Trend analysis of rainfall in the  
533 headstreams of the Zambezi River Basin in Zambia. *Phys. Chem. Earth.*, 33,  
534 621-625, doi:10.1016/j.pce.2008.06.012, 2008.
- 535 Krupa, S. V.: Effects of atmospheric ammonia (NH<sub>3</sub>) on terrestrial vegetation: a review,  
536 *Environ. Pollut.*, 124, 179-221, doi:10.1016/S0269-7491(02)00434-7, 2003.





- 537 Kulmala, M., Vehkamäki, H., Petäjä, T., Dal Maso, M., Lauri, A., Kerminen, V., Birmili,  
538 W., McMurry, P. H.: Formation and growth rates of ultrafine atmospheric  
539 particles: a review of observations, *J. Aerosol. Sci.*, 35, 143-176,  
540 DOI:10.1016/j.jaerosci.2003.10.003, 2004.
- 541 Lillyman, C., Buset, K., and Mullins, D.: Canadian Atmospheric Assessment of  
542 Agricultural Ammonia, National Agri-Environmental Standards, Environment  
543 Canada, Gatineau, Quebec, 2009.
- 544 Markovic, M. Z., VandenBoer, T. C., Baker, K. R., Kelly, J. T., Murphy, J. G.:  
545 Measurements and modeling of the inorganic chemical composition of fine  
546 particulate matter and associated precursor gases in California's San Joaquin  
547 Valley during CalNex 2010, *J. Geophys. Res.-Atmos.*, 119, 6853-6866,  
548 doi:10.1002/2013JD021408, 2014.
- 549 Meng, Z. Y., Lin, W. L., Jiang, X. M., Yan, P., Wang, Y., Zhang, Y. M., Jia, X. F., Yu, X.  
550 L.: Characteristics of atmospheric ammonia over Beijing, China, *Atmos. Chem.*  
551 *Phys.*, 11, 6139-6151, doi:10.5194/acp-11-6139-2011, 2011.
- 552 Nowak, J. B., Neuman, J. A., Bahreini, R., Middlebrook, A. M., Holloway, J. S.,  
553 McKeen, S. A., Parrish, D. D., Ryerson, T. B., Trainer, M.: Ammonia sources in  
554 the California South Coast Air Basin and their impact on ammonium nitrate  
555 formation, *Geophys. Res. Lett.*, 39, L07804, doi:10.1029/2012GL051197, 2012.
- 556 Paulot, F. and Jacob, D. J.: Hidden cost of US agricultural exports: particulate matter  
557 from ammonia emissions. *Environ. Sci. Technol.*, 48, 903-908,  
558 doi:10.1021/es4034793, 2014.
- 559 Pinder, R. W., Davidson, E. A., Goodale, C. L., Greaver, T. L., Herrick, J. D., Liu, L.:  
560 Climate change impacts of US reactive nitrogen, *Proc. Nat. Acad. Sci. USA.*, 109,  
561 7671-7675, doi:10.1073/pnas.1114243109, 2012.
- 562 Puchalski, M. A., Rogers, C. M., Baumgardner, R., Mishoe, K. P., Price, G., Smith, M.  
563 J., Watkins, N., Lehmann, C. M.: A statistical comparison of active and passive  
564 ammonia measurements collected at Clean Air Status and Trends Network  
565 (CASTNET) sites, *Environ. Sci-Proc. Imp.*, 17, 358-369,  
566 doi:10.1039/c4em00531g, 2015.
- 567 Pugliese, S. C., Murphy, J. G., Geddes, J. A., Wang, J. M.: The impacts of precursor  
568 reduction and meteorology on ground-level ozone in the Greater Toronto Area,  
569 *Atmos. Chem. Phys.*, 14, 8197-8207, doi:10.5194/acp-14-8197-2014, 2014.
- 570 Pye, H., Liao, H., Wu, S., Mickleby, L. J., Jacob, D. J., Henze, D. K., Seinfeld, J. H.:  
571 Effect of changes in climate and emissions on future sulfate-nitrate-ammonium  
572 aerosol levels in the United States, *J. Geophys. Res.-Atmos.*, 114, D01205,  
573 doi:10.1029/2008JD010701, 2009.
- 574 Reche, C., Viana, M., Pandolfi, M., Alastuey, A., Moreno, T., Amato, F., Ripoll, A.,  
575 Querol, X.: Urban NH<sub>3</sub> levels and sources in a Mediterranean environment,  
576 *Atmos. Environ.*, 57, 153-164, doi:10.1016/j.atmosenv.2012.04.021, 2012.



- 577 Ren, H., Wang, Y., Huang, M., Chang, Y., Kao, H.: Ensemble empirical mode  
578 decomposition parameters optimization for spectral distance measurement in  
579 hyperspectral remote sensing data, *Remote Sens.-Basel.*, 6, 2069-2083,  
580 doi:10.3390/rs6032069, 2014.
- 581 Saylor, R. D., Edgerton, E. S., Hartsell, B. E., Baumann, K., Hansen, D. A.: Continuous  
582 gaseous and total ammonia measurements from the southeastern aerosol research  
583 and characterization (SEARCH) study, *Atmos. Environ.*, 44, 4994-5004,  
584 doi:10.1016/j.atmosenv.2010.07.055, 2010.
- 585 Schiferl, L. D., Heald, C. L., Nowak, J. B., Holloway, J. S., Neuman, J. A., Bahreini, R.,  
586 Pollack, I. B., Ryerson, T. B., Wiedinmyer, C., Murphy, J. G.: An investigation of  
587 ammonia and inorganic particulate matter in California during the CalNex  
588 campaign, *J. Geophys. Res.-Atmos.*, 119, 1883-1902,  
589 doi:10.1002/2013JD020765, 2014.
- 590 Su, H., Cheng, Y., Oswald, R., Behrendt, T., Trebs, I., Meixner, F. X., Andreae, M. O.,  
591 Cheng, P., Zhang, Y., Pöschl, U.: Soil nitrite as a source of atmospheric HONO  
592 and OH radicals, *Science*, 333(6049), 1616-1618, doi:10.1126/science.1207687,  
593 2011.
- 594 Sutton, M. A., Nemitz, E., Theobald, M. R., Milford, C., Dorsey, J. R., Gallagher, M.  
595 W., Hensen, A., Jongejan, P., Erisman, J. W., Mattsson, M.: Dynamics of  
596 ammonia exchange with cut grassland: strategy and implementation of the  
597 GRAMINAE Integrated Experiment, *Biogeosciences*, 6, 309-331,  
598 doi:10.5194/bg-6-309-2009, 2009.
- 599 Sutton, M. A., Reis, S., Riddick, S. N., Dragosits, U., Nemitz, E., Theobald, M. R.,  
600 Tang, Y. S., Braban, C. F., Vieno, M., Dore, A. J.: Towards a climate-dependent  
601 paradigm of ammonia emission and deposition, *Philos. T. Roy. Soc. B.*, 368,  
602 20130166, doi:10.1098/rstb.2013.0166, 2013.
- 603 Theobald, M. R., Løfstrøm, P., Walker, J., Andersen, H. V., Pedersen, P., Vallejo, A.,  
604 Sutton, M. A.: An intercomparison of models used to simulate the short-range  
605 atmospheric dispersion of agricultural ammonia emissions, *Environ. Modell.*  
606 *Softw.*, 37, 90-102, doi:10.1016/j.envsoft.2012.03.005, 2012.
- 607 Van Damme, M., Clarisse, L., Heald, C. L., Hurtmans, D., Ngadi, Y., Clerbaux, C.,  
608 Dolman, A. J., Erisman, J. W., Coheur, P. F.: Global distributions, time series and  
609 error characterization of atmospheric ammonia (NH<sub>3</sub>) from IASI satellite  
610 observations, *Atmos. Chem. Phys.*, 14 (6), 2905-2922,  
611 doi:10.5194/acp-14-2905-2014, 2014.
- 612 Walker, J.T., Aneja V.P., Dickey D.A.: Atmospheric transport and wet deposition of  
613 ammonium in North Carolina, *Atmos. Environ.*, 34, 3407-3418,  
614 doi:10.1016/S1352-2310(99)00499-9, 2000.
- 615 Walker, J. M., Philip, S., Martin, R. V., Seinfeld, J. H.: Simulation of nitrate, sulfate,  
616 and ammonium aerosols over the United States, *Atmos. Chem. Phys.*, 12,  
617 11213-11227, doi:10.5194/acp-12-11213-2012, 2012.



- 618 Whitehead, J. D., Longley, I. D., Gallagher, M. W.: Seasonal and diurnal variation in  
619 atmospheric ammonia in an urban environment measured using a quantum  
620 cascade laser absorption spectrometer, *Water Air Soil Pollut.*, 183, 317-329,  
621 doi:10.1007/s11270-007-9381-5, 2007.
- 622 Wu, Z. and Huang, N. E.: Ensemble empirical mode decomposition: a noise-assisted  
623 data analysis method, *Adv. Adapt. Data Anal.*, 1, 1-41, 2009.
- 624 Xing, J., Pleim, J., Mathur, R., Pouliot, G., Hogrefe, C., Gan, C.-M., Wei, C.:  
625 Historical gaseous and primary aerosol emissions in the United States from  
626 1990 to 2010, *Atmos. Chem. Phys.*, 13, 7531-7549,  
627 doi:10.5194/acp-13-7531-2013, 2013.
- 628 Yao, X. H. and Zhang, L.: Supermicron modes of ammonium ions related to fog in rural  
629 atmosphere, *Atmos. Chem. Phys.*, 12, 11165-11178,  
630 doi:10.5194/acp-12-11165-2012, 2012.
- 631 Yao, X., Hu, Q., Zhang, L., Evans, G.J., Godri, K.J., Ng, A.C.: Is vehicular emission a  
632 significant contributor to ammonia in the urban atmosphere?, *Atmos. Environ.*,  
633 80, 499-506, doi:10.1016/j.atmosenv.2013.08.028, 2013.
- 634 Yao, X. H. and Zhang, L.: Analysis of passive-sampler monitored atmospheric  
635 ammonia at 74 sites across southern Ontario, Canada, *Biogeosciences*, 10,  
636 7913-7925, doi:10.5194/bg-10-7913-2013, 2013.
- 637 Zbieranowski, A. L. and Aherne, J.: Long-term trends in atmospheric reactive nitrogen  
638 across Canada: 1988-2007, *Atmos. Environ.*, 45, 5853-5862,  
639 doi:10.1016/j.atmosenv.2011.06.080, 2011.
- 640 Zhang, L., Wright, L. P., Asman, W.: Bi-directional air-surface exchange of  
641 atmospheric ammonia: A review of measurements and a development of a  
642 big-leaf model for applications in regional-scale air-quality models, *J. Geophys.*  
643 *Res.-Atmos.*, 115, D20310, doi:10.1029/2009JD013589, 2010.
- 644 Zhu, L., Henze, D. K., Cady Pereira, K. E., Shephard, M. W., Luo, M., Pinder, R. W.,  
645 Bash, J. O., Jeong, G. R.: Constraining US ammonia emissions using TES remote  
646 sensing observations and the GEOS-Chem adjoint model, *J. Geophys.*  
647 *Res.-Atmos.*, 118, 3355-3368, doi:10.1002/jgrd.50166, 2013.

648

649

650 Table 1. The mixing ratios of atmospheric NH<sub>3</sub> at fourteen sites (NH<sub>3</sub> unit in ppb, T unit in °C, Sites 1-14 were defined in the text)

Site	Sampling Period	Annual			Spring		Summer		Fall		Winter	
		NH <sub>3</sub>	NH <sub>3</sub>	T	NH <sub>3</sub>	T	NH <sub>3</sub>	T	NH <sub>3</sub>	T	NH <sub>3</sub>	T
1	July. 2003-June. 2014	2.6±1.2	2.8±1.2	8.0±6.0	3.7±0.7	21.6±1.5	2.8±0.7	11.8±5.7	1.3±0.6	-2.5±3.1		
2	May. 2006-Apr. 2014	2.4±0.6	2.3±0.6	3.7±7.4	2.4±0.4	16.7±1.9	2.6±0.6	4.2±7.7	2.3±0.9	-19.8±4.5		
3	Sep. 2003-Aug. 2014	2.1±2.0	1.6±0.8	6.1±6.7	3.0±1.5	19.5±2.2	3.2±2.8	9.1±5.6	0.5±0.3	-6.8±2.9		
4	Nov. 2007-Oct. 2014	1.9±0.8	1.7±0.7	8.3±6.9	2.7±0.5	21.5±2.1	2.1±0.4	9.4±6.3	1.0±0.2	-6.1±2.6		
5	Sep. 2003-Aug. 2014	1.6±0.5	1.5±0.4	10.1±2.9	1.9±0.4	17.8±1.9	1.7±0.5	10.6±4.1	1.4±0.4	4.2±1.5		
6	Aug. 2003-July 2011	0.8±0.6	1.0±0.7	6.7±5.8	1.2±0.4	19.4±2.2	0.7±0.3	9.7±5.3	0.2±0.2	-5.6±2.8		
7	Aug. 2008-July. 2015	4.9±1.2	4.6±1.2	14.2±4.2	5.5±0.8	25.5±1.7	4.7±1.5	14.7±5.3	4.6±1.4	3.0±1.8		
8	Aug. 2008-July. 2015	2.6±1.4	3.2±1.2	7.4±6.5	3.8±0.9	20.7±1.8	2.5±0.6	9.3±5.9	1.0±0.5	-7.4±3.8		
9	Aug. 2008-July. 2015	2.2±1.0	2.6±1.0	10±6.1	3.2±0.7	22.4±1.7	2.1±0.7	11.5±5.5	1.1±0.3	-3.2±3.3		
10	Aug. 2008-July. 2015	1.6±1.0	2.3±1.0	11.3±5.7	1.9±0.4	22.1±1.5	1.8±0.8	11.2±5.6	0.4±0.4	-3.3±3.3		
11	Aug. 2008-July. 2015	0.5±0.4	0.7±0.4	6.6±6.5	0.8±0.3	18.4±1.5	0.3±0.2	9.2±5.0	0.1±0.1	-4.9±3.4		
12	Sep. 2008-Aug. 2015	0.3±0.3	0.3±0.2	3.4±6.1	0.5±0.3	17.5±2.6	0.3±0.3	5.5±6.7	0.1±0.1	-13±4.5		
13	Aug. 2008-July. 2015	0.3±0.4	0.2±0.2	11±3.6	0.7±0.5	23.8±1.5	0.2±0.2	12.5±6.0	0.2±0.1	0.2±2.3		
14	Aug. 2008-July. 2015	0.3±0.3	0.4±0.2	18.6±4.2	0.5±0.3	27.8±1.0	0.2±0.2	19.7±4.8	0.2±0.2	10.3±3.2		

651



652

653 **List of Figures**

654

655 Fig. 1 Map of fourteen long-term atmospheric NH<sub>3</sub> monitoring sites across North  
656 America.

657 Fig. 2 Monthly averages of atmospheric NH<sub>3</sub> measured at six Canadian sites.

658 Fig. 3 Monthly averages of atmospheric NH<sub>3</sub> measured at eight U.S. sites.

659 Fig. 4 Correlations between atmospheric NH<sub>3</sub> and ambient T at Site 1 (a: annual  
660 average value; b: EEMD-extracted trend).

661 Fig. 5 The long-term trends in atmospheric NH<sub>3</sub> extracted by the EEMD at six  
662 Canadian sites.

663 Fig. 6 The long-term trends in atmospheric NH<sub>3</sub> extracted by the EEMD at eight U.S.  
664 sites.

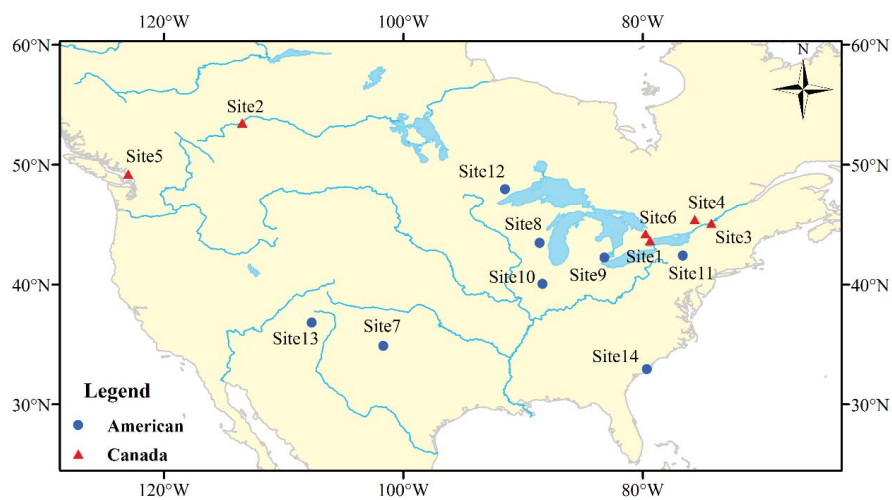
665

666

667



668 Fig 1



669

670

671

672

673

674

675

676

677

678

679

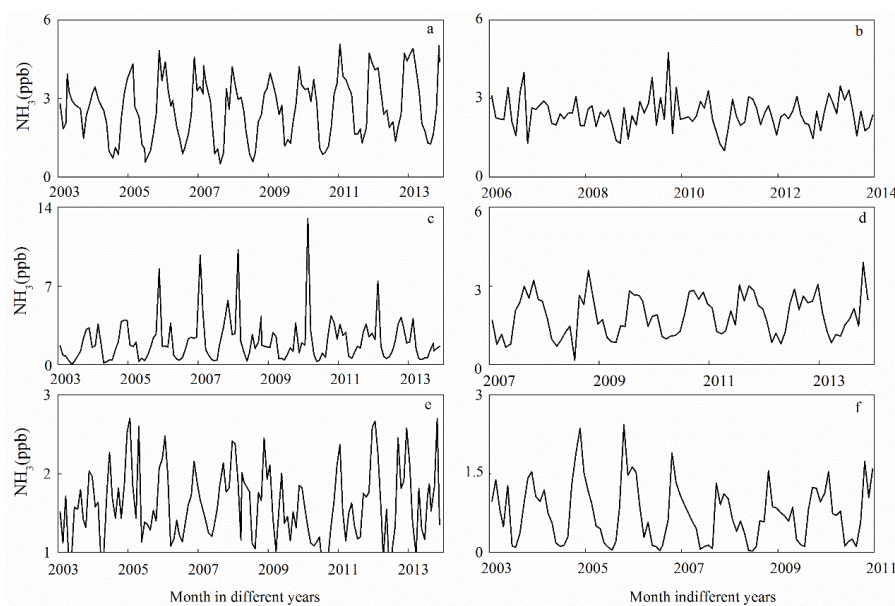
680

681

682



683 Fig 2



684

685

686

687

688

689

690

691

692

693

694

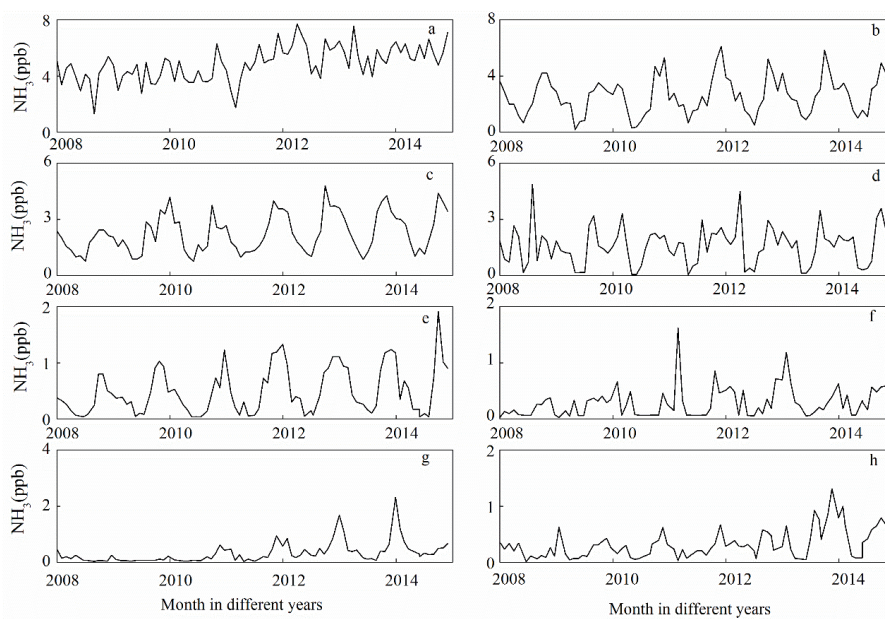
695

696



697

698 Fig 3



699

700

701

702

703

704

705

706

707

708

709

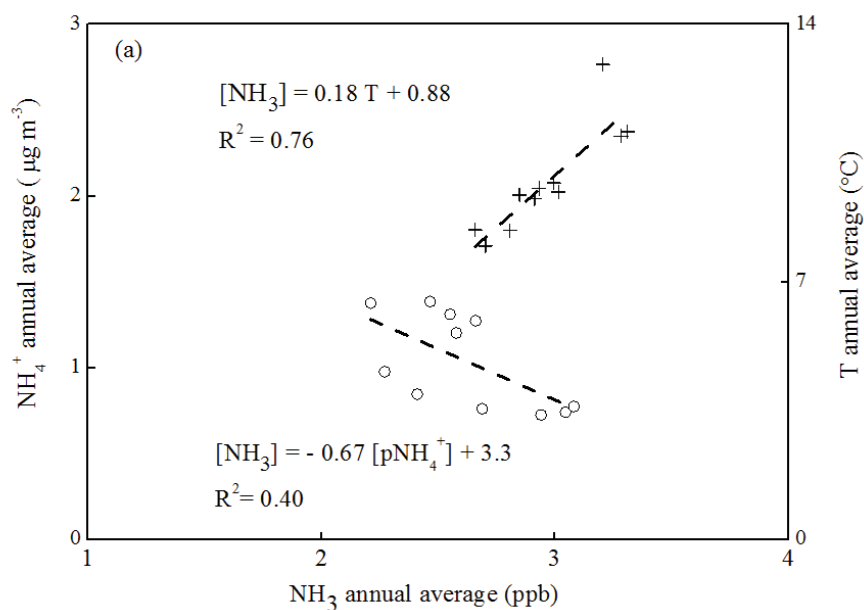
710



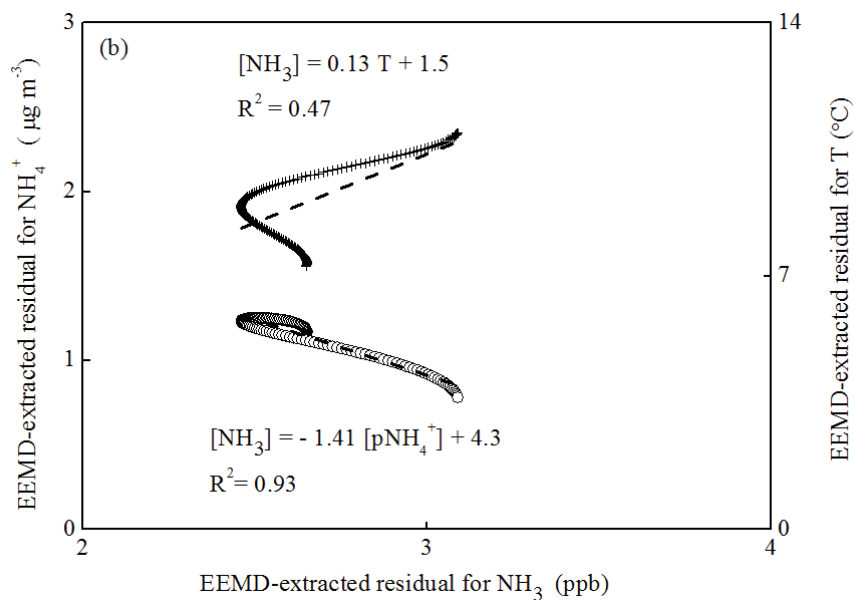


711

712 Fig 4



713



714

715

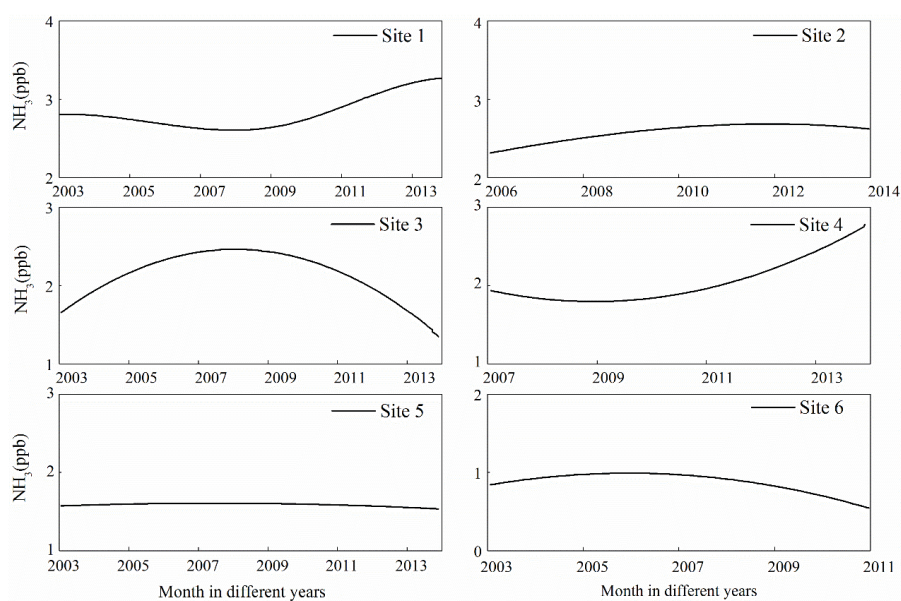


716

717

718 Fig 5

719



720

721

722

723

724

725

726

727

728

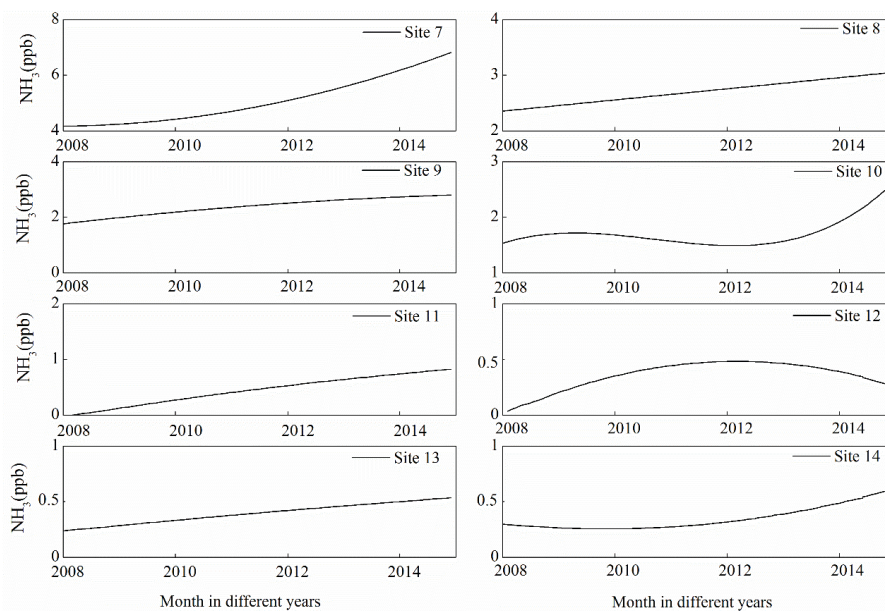
729



730

731

732 Fig 6



733

734

735

736